J Neurophysiol 96: 2282–2294, 2006.
First published August 2, 2006; doi:10.1152/jn.00078.2006.

NMDA Receptor Subtypes at Autaptic Synapses of Cerebellar Granule Neurons

Congyi Lu,[1] Zhanyan Fu,[1] Irina Karavanov,[3] Robert P. Yasuda,[2] Barry B. Wolfe,[2] Andres Buonanno,[3] and Stefano Vicini[1]

[1]*Department of Physiology and Biophysics and* [2]*Department of Pharmacology, Georgetown University School of Medicine, Washington, DC; and* [3]*Section on Molecular Neurobiology, National Institute of Child Health and Human Development, National Institutes of Health, Bethesda, Maryland*

Submitted 24 January 2006; accepted in final form 17 July 2006

Lu, Congyi, Zhanyan Fu, Irina Karavanov, Robert P. Yasuda, Barry B. Wolfe, Andres Buonanno, and Stefano Vicini. NMDA receptor subtypes at autaptic synapses of cerebellar granule neurons. *J Neurophysiol* 96: 2282–2294, 2006. First published August 2, 2006; doi:10.1152/jn.00078.2006. We studied the action potential–evoked autaptic *N*-methyl-D-aspartate receptor-mediated excitatory postsynaptic currents (NMDA-EPSCs) using solitary cerebellar neurons cultured in microislands from wild-type (+/+), NR2A subunit knockout (NR2A−/−), and NR2C subunit knockout (NR2C−/−) mice. The peak amplitude of autaptic NMDA-EPSCs increased for all genotypes between days in vitro 8 (DIV8) and DIV13. Compared with +/+ cells at DIV13, NR2A−/− cells had smaller and NR2C−/− cells had larger NMDA-EPSCs. The decay time of these currents were all unexpectedly fast, except in NR2A−/− neurons, and showed small but significant shortening with development. Comparison of quantal parameters during development indicated an increase in quantal content in all genotypes. The synaptic portion of NMDA receptors measured using MK-801 blockade was roughly 50% in all genotypes at DIV8, and this percentage became slightly larger in NR2A−/− and NR2C−/− neurons at DIV12. The NR2B-selective antagonists Conantokin G and CP101,606 differed in their blocking actions with development, suggesting the presence of both heterodimeric NR1/NR2B and heterotrimeric NR1/NR2A/NR2B receptors. The most striking result we obtained was the significant increase of NMDA-EPSC peak amplitude and charge transfer in NR2C−/− mice. This was mainly the result of an increase in quantal size as estimated from miniature NMDA-EPSCs. The expression of NR2C subunit containing receptors was supported by the decreased Mg^{2+} sensitivity of NMDA receptors at DIV13 in +/+ but not in NR2C−/− cells. Thus solitary cerebellar granule neurons provide a novel model to investigate the role of receptor subtypes in the developmental changes of synaptic NMDA receptors.

INTRODUCTION

Solitary neurons plated on substrate microislands can form functional autapses that are similar to synapses in high-density mass cultures and that are amenable to electrophysiological studies (Bekkers and Stevens 1991; Mennerick et al. 1994). They offer advantages over brain slices and mass cell cultures to study neurotransmitter release because the sources of synaptic input are homogeneous and originate from the same neuron. Thus the evoked and spontaneous release can be recorded from the same synapses. Using this model system, several aspects of excitatory synaptic transmission have been studied, such as the relative distribution of synaptic and extrasynaptic *N*-methyl-D-aspartate (NMDA) receptors (Li et al. 2002; Rosenmund et al. 1993; Thomas et al. 2006; Tovar and Westbrook 1999). A critical role of metabotropic glutamate receptor and a unique pre- and postsynaptic coupling for maturation of hippocampal synapse (Chavis and Westbrook 2001; Gomperts et al. 2000) were elucidated from autapses. The occurrence of pre- and postsynaptically silent synapses (Gomperts et al. 1998; Kimura et al. 1997) was also reported for solitary neurons. Furthermore, activity-dependent maturation, synaptic plasticity, and the role of neurotrophins were elucidated using autaptic neurons (Kumura and Tsumoto 2000; Takada et al. 2005). However, all of these studies used neurons from either hippocampus or cortex. Here, we report the study of cultured solitary neurons from cerebellum for the first time.

Because primary cultures from postnatal cerebellum of rodents are principally composed of excitatory glutamatergic granule cells (roughly 95%) and a few GABAergic interneurons (stellate, basket, and Golgi neurons), either solitary cerebellar granule cells (CGCs) or GABAergic interneurons can be formed in these culture conditions. In solitary CGCs, the presynaptic site is the same as the output of the parallel fiber to Purkinje neurons in vivo, which uses glutamate as the neurotransmitter and the postsynaptic site is the same as that of the mossy fiber–granule cell relay. Previous work revealed that mossy fiber–granule cell synaptic transmission is mediated by NMDA as well as non-NMDA receptors (Garthwaite and Brodbelt 1990) in the mature cerebellum, whereas in immature cerebellum they are predominantly mediated by NMDA receptors (D'Angelo et al. 1993).

NMDA receptors are formed by the assembly of multiple NR1 subunits and at least one of NR2 subunit types (for review see Cull-Candy et al. 2001). In the cerebellum, NR2B subunit mRNA and protein expression begin in late embryonic stages and then decrease during the second postnatal week. In contrast, NR2A subunit expression begins postnatally during migration of granule cell to the internal granular layer followed by NR2C subunit expression (Takahashi et al. 1996; Wang et al. 1995; Watanabe et al. 1994). Recombinant NMDA receptors composed of NR1/NR2B and NR1/NR2C subunits are characterized by slow deactivation kinetics, whereas NR1/NR2A channels are characterized by faster kinetics (Monyer et al. 1994; Vicini et al. 1998). Indeed, the kinetics of NMDA–excitatory postsynaptic currents (EPSCs) become faster after the second postnatal week (Cathala et al. 2000; Rumbaugh and Vicini 1999) and then slow again later in life when the NR2C subunit expression increases (Cathala et al. 2000). These

Address for reprint requests and other correspondence: S. Vicini, Department of Physiology and Biophysics, BSB225, Georgetown University School of Medicine, 3900 Reservoir Rd., Washington, DC 20007 (E-mail: svicin01@georgetown.edu).

The costs of publication of this article were defrayed in part by the payment of page charges. The article must therefore be hereby marked "*advertisement*" in accordance with 18 U.S.C. Section 1734 solely to indicate this fact.

changes are significantly altered in mice lacking specific NR2 subunits (Ebralidze et al. 1996; Takahashi et al. 1996).

Using cultures of solitary cerebellar neuron from wild-type (+/+), NR2A knockout (NR2A−/−), and NR2C knockout (NR2C−/−) mice, we investigated whether the changes observed in vivo can be reproduced with this in vitro model. Cerebellar granule cells have small somatic size and a few dendrites per cell. This makes comparison of NMDA-EPSCs between genotypes appealing because channel currents can be recorded with high resolution under ideal voltage-clamp conditions (Silver et al. 1992).

The present results extend previous work on the changes in functional and pharmacological properties of synaptic NMDA receptors in high-density cerebellar granule cell cultures (Fu et al. 2005) to autaptic synapses of solitary cerebellar granule neurons from different genotypes. This model allowed us to determine the influence of specific NR2 subunit on the properties and the formation of excitatory synapses with age in vitro.

METHODS

Wild-type, NR2A−/−, and NR2C−/− mice

In this study we used C57BL/6J, strain 129/Sv/SvJ, as wild-type control mice. NR2A−/− (ε1−/−) mice are described in Takahashi et al. 1996. We generated NR2C−/− (ε3−/−) mice with a homologous recombination targeting vector that was constructed to insert a nuclear β-galactosidase reporter gene in frame with the initiator methionine of the NMDA receptor NR2C subunit and to remove the first 11 exons of the gene (Karavanova and Buonanno, unpublished data). The targeting vector was transfected into TC-1 ES cells (129Sv/Ev derived) by electroporation. The DNA construct harbored pGK-neo (floxed) and pGK-tk herpes virus expression cassettes used for the positive and negative screening of recombinant embryonic stem (ES) cells, respectively. Proper homologous recombination of the left and right arms were screened and confirmed by restriction digests and Southern blot analysis. Positive ES cell clones were microinjected into C57BL/6 blastocysts. The pGK-neo cassette was removed subsequently by crossing the NR2C-β-gal mice to a transgenic cre recombinase line driven by the E2a promoter. All mouse procedures were performed in compliance with the National Institutes of Health Guide for the Care and Use of Laboratory Animals and the Georgetown University Institutional Animal Care and Use Committee.

Solitary cerebellar neuron cultures

Solitary neuron cultures were made using the method adapted from microisland hippocampal cultures described previously (Bekkers and Stevens 1991). Briefly, 12-mm glass coverslips (Fisher Scientific, Pittsburgh, PA) were coated with 0.15% agarose (Sigma, St. Louis, MO) and allowed to dry. A solution of poly-D-lysine (0.5 mg/ml, Sigma) was then sprayed on the agarose background to form microdots. The cerebella from day 5–day 7 mice were removed, enzymatically and mechanically dissociated, and then plated on previously prepared coverslips that were already transferred to 35-mm Nunc dishes (Fisher Scientific) with glial feeder layers. The cells were cultured in basal Eagle's medium supplemented with 10% fetal bovine serum, 2 mM glutamine, and 100 μg/ml gentamycin (all from Invitrogen, Carlsbad, CA), and maintained at 37°C in 5% CO_2. The final concentration of KCl in the culture medium was adjusted to 25 mM. At DIV5 the medium was replaced with 5 mM K^+ medium (MEM) supplemented with 5 mg/ml glucose, 0.1 mg/ml transferrin, 0.025 mg/ml insulin, 2 mM glutamine, and 20 μg/ml gentamycin (Invitrogen).

Electrophysiology

Whole cell voltage-clamp recordings were performed on mouse cerebellar neurons in microisland cultures after ≥7 days in vitro. All recordings were done at room temperature (23–25°C). Continuously perfused extracellular solution contained (in mM): NaCl (145), KCl (5), $MgCl_2$ (1), $CaCl_2$ (1), HEPES (5), glucose (5), sucrose (15), phenol red (0.25 mg/l), and D-serine (10 μM) adjusted to pH 7.4 with NaOH. Electrodes were filled with recording solution containing (in mM): K-gluconate (145), HEPES (10), ATP-Mg (5), GTP-Na (0.2), and EGTA (1.1), adjusted to pH 7.2 with KOH. Whole cell voltage-clamp recordings were made at −70 mV with an Axopatch-1D amplifier and access resistance was monitored throughout the recordings. Currents were filtered at 1 kHz with an eight-pole low-pass Bessel filter and digitized at 5–10 kHz using an IBM-compatible microcomputer equipped with Digidata 1322A data acquisition board and pCLAMP9 software. Autaptic EPSCs were evoked with a depolarizing step (to +10 mV, 0.5 ms) at 0.2 Hz. Stock solutions of NMDA (Sigma), bicuculline metabromide (BMR, Sigma), tetrodotoxin (TTX, Alomone Labs, Israel), 3-[(±)-2-carboxypiperazin-4-yl]-propyl-1-phosphonic acid (CPP, Tocris Cookson, Ballwin MO), 2,3-dihydro-6-nitro-7-sulfamoyl-benzo(F)quinoxaline (NBQX, Tocris), and Conantokin G (a gift from Drs. Mary Prorok and Frank Castellino, Department of Chemistry and Biochemistry, University of Notre Dame, Notre Dame, IN) were dissolved in water. CP101,606 {(1S,2S)-1-(4-hydroxyphenyl)-2-(4-hydroxy-4-phenylpiperidino)-1-propanol, a gift from Dr. Richard Woodward, Acea Pharmaceutical, Irvine, CA)} and MK-801 maleate (Dizocilpine, Tocris) were dissolved in dimethylsulfoxide (DMSO, <0.1% final concentration). Drugs were diluted in the Mg^{2+}-free extracellular medium and applied with a Y-tube (Murase et al. 1989). NMDA was applied in Ca^{2+}- and Mg^{2+}-free extracellular medium to prevent Ca^{2+}-mediated inactivation.

Autaptic EPSC averages were based on ≥20 consecutive events in each cell studied. Decay times of averaged currents derived from fitting using a simplex algorithm for least-squares exponential fitting routines to double-exponential equations of the form $I(t) = I_f \times \exp(-t/\tau_f) + I_s \times \exp(-t/\tau_s)$, where I_f and I_s are the amplitudes of the fast and slow decay components and τ_f and τ_s are their respective decay time constants used to fit the data. To compare decay times, we used a weighted mean decay time constant $\tau_w = [I_f/(I_f + I_s)] \times t_f + [I_s/(I_f + I_s)] \times t_s$. Synaptic charge transfer (Q) was determined from the area underlying the EPSC $Q = I \times \tau_w$. All data are expressed as means ± SE; P values represent the results of two-tailed unpaired Student's t-test assuming homogeneity of variances with Bonferroni corrections when needed.

Immunocytochemistry

All immunostaining experiments were carried out at room temperature. Neurons were fixed by incubation with 4% paraformaldehyde, 4% sucrose in phosphate-buffered saline (PBS) for 5 min, and washed three times in PBS. Fixed neurons were permeabilized with 0.3% Triton X-100/PBS for 5 min, washed several times with PBS, and incubated in 10% bovine serum albumin in PBS for 1 h to block nonspecific staining. Cells were then incubated for 1 h with one of the following primary antibodies: rabbit anti-synapsin (1 μg/ml, Chemicon, Temecula, CA) or anti-Bassoon (3 μg/ml, Stressgen, San Diego, CA). After washing with PBS, cells were incubated with indocarbocyanine (Cy3)-conjugated secondary antibodies (1:1,000, Jackson ImmunoResearch Laboratories, West Grove, PA) or with Alexa 488–conjugated secondary antibodies (1:400, Molecular Probes, Eugene, OR).

Stained neurons were imaged on a Nikon E600 microscope (Nikon, Tokyo, Japan) equipped with a ×40 and ×60, 1.0 N.A. water-immersion objective. Digital images were acquired with a CFW-1310 (Scion, Frederick, MD), 10-bit (1,024 gray-scale intensity level) CCD digital camera, 1,360 × 1,024 pixel array. For a given antibody stain,

images were acquired using identical parameters. The 8-bit images were analyzed blindly with MetaMorph (Universal Imaging, Downingtown, PA) after background subtraction of camera noise and flatfield division to level the intensity. Images were pseudocolored for presentation with Adobe Photoshop 7.0 (Adobe, San Jose, CA).

Antibody-positive clusters were defined and counted as clusters of fluorescence that were at least twice the background fluorescence of the image. The cluster size limitation was set by the autoregion selection (0.5 × 0.5 μm) by using MetaMorph software.

All data are expressed as means ± SE; *P* values represent the results of two-tailed unpaired Student's *t*-test.

Western blot analysis

Samples were diluted in loading buffer, and then SDS gel electrophoresis was performed by applying each sample to a 7.5% acrylamide gel. Proteins were transferred to PVDF membrane, blocked with 1% bovine serum albumin (BSA) in TBST (20 mM Tris-HCl, pH 7.6, 137 mM NaCl, 0.1% Tween-20), and probed with specific NMDA receptor subunit antibodies in 1% BSA in TBST at 4°C overnight with gentle rocking. The NR2A, NR2B, NR2C, NR2D, and NR3A antibodies were rabbit polyclonal antibodies that were affinity purified and each used at a concentration of 1 μg/ml (Al-Hallaq et al. 2002; Dunah et al. 1996; Wang et al. 1995). The NR1 antibody (Luo et al. 1997), a mouse monoclonal antibody, was also used at a concentration of 1 μg/ml. Primary antibodies were removed and immunoblots washed with TBST, then incubated with the appropriate HRP-conjugated secondary antibody for 30 min after three washes with TBST. The immunoblots were incubated with West-Pico chemiluminiscent reagents (Pierce Biotechnology, Rockford, IL) for 5 min and then placed against Hyperfilm-MP (GE Healthcare Bio-Sciences, Piscataway, NJ) for varying times. Film densitometry was analyzed with Intelligent Quantifier software (BioImage, Ann Arbor, MI).

RESULTS

Autaptic EPSCs recorded from solitary CGCs

Microisland cultures of cerebellar neurons were prepared using the procedure adapted from microisland hippocampal cultures (Bekkers and Stevens 1991), as described in more detail in METHODS. The majority of microislands contained two or more neurons. However, several had single neurons, either a glutamatergic granule neuron, identified from the cell body diameter of ≤7 μm (Fig. 1*A*, *left*), or a GABAergic interneuron that displayed a larger cell body (Fig. 1*B*, *left*). Because the axons of neurons were constrained to grow within a small region, they normally grew in circular loops and formed autaptic connections with their own dendrites and cell bodies.

Cultures were studied 7 days after plating the neurons and 2 days after changing the culture medium to low potassium, a culture condition that favors the formation of functional synapses (Chen et al. 2000). Using whole cell voltage-clamp recordings, autaptic currents could be elicited in solitary neurons after a brief depolarization. Functional autaptic connections were found in all cells studied from cultures older than 7 days in vitro (>140 neurons from 16 distinct culture preparations). Cerebellar granule neurons (CGCs) showed fast excitatory autaptic currents, which could be antagonized by the α-amino-3-hydroxy-5-methyl-4-isoxazolepropionic acid (AMPA)–receptor-selective blocker NBQX (Fig. 1*A*, *right*), whereas interneurons showed slower inhibitory autaptic currents that were blocked by BMR (Fig. 1*B*, *right*).

As illustrated in Fig. 1*C*, when Mg^{2+} (1 mM) was removed from the extracellular recording solution, the autaptic EPSCs recorded from the CGCs (*top*, *left*, *gray trace*) became larger and long-lasting (*top*, *middle*, *black trace*). Application of the NMDA-receptor antagonist CPP inhibited the long-lasting current, leaving the AMPA-receptor–mediated EPSCs (AMPA-EPSCs) (*top*, *right*, *gray trace*). As seen in the expanded traces (Fig. 1*C*, *bottom*, *right*), the AMPA-EPSC decayed before the peak of the NMDA-receptor–mediated EPSC (NMDA-EPSCs). In a few cells, the amplitude and decay of NMDA-EPSCs recorded in the presence and the absence of NBQX were compared, and no differences were found under these two conditions. Thus for the majority of the subsequent experiments in this study, an AMPA-receptor antagonist was not used to pharmacologically isolate NMDA-EPSCs.

For all the autaptic EPSCs investigated, averages of consecutive currents were fitted by double-exponential curves to measure the peak amplitude (*I*) and weighted time constant of decay (τ_w) (see METHODS). Both in the presence and the absence of Mg^{2+}, double exponentials were needed to best describe these currents. The fast decay component in the presence of Mg^{2+} was selected to estimate the AMPA-EPSCs to exclude the contribution of NMDA-EPSCs (<15%). Instead, both fast and slow components were used to measure the NMDA-EPSCs in the absence of Mg^{2+} (Fig. 1*D*, *right*). The EPSCs recorded from the same cell were stable over recording time. In three cells, the amplitude and decay of the average of 10 consecutive NMDA-EPSCs remained constant for over 30 min, although with considerable variability of each individual sweep from the average.

Differences in NMDA-EPSCs and AMPA-EPSCs in solitary CGCs from +/+, NR2A−/−, and NR2C−/− mice at distinct ages in vitro

To investigate the role of different NR2 subunits on synapse formation and the properties of EPSCs, we compared autaptic NMDA-EPSCs and AMPA-EPSCs recorded from +/+, NR2A−/−, and NR2C−/− solitary CGCs kept in culture from 8 to 13 days in vitro (DIV). Sample traces of autaptic NMDA-EPSCs recorded at DIV8 and DIV13 are shown in Fig. 2*A*. The peak amplitude of autaptic NMDA-EPSCs showed similar increased trends with development for all genotypes. However, autaptic NMDA-EPSCs were significantly smaller in NR2A−/− cells than in +/+ cells at all ages examined, whereas in NR2C−/− cells they showed significantly increased peak amplitude only at later ages (DIV13, Fig. 2*B*, *left*). This suggested that the presence of NR2A or NR2C subunit regulated the peak amplitude of NMDA-EPSCs in opposite directions.

Generally, the decay time constants (τ_w) of NMDA-EPSCs at DIV8–9 in +/+ solitary neurons (Fig. 2*B*, *right*) were faster compared with those of miniature NMDA-EPSCs recorded from mass cerebellar cultures (Fu et al. 2005; Pryblowski et al. 2002) as well as cerebellar slices at comparable developmental stages (Cathala et al. 2000; Ebralidze et al. 1996; Rumbaugh et al. 1999; Takahashi et al. 1996). In a comparison of genotypes, the NMDA-EPSCs from +/+ cells and NR2C−/− cells were remarkably faster than those from NR2A−/− cells at all age groups examined and became slightly but significantly faster from DIV8 to DIV13. These data were consistent with our previous findings that NR2A-containing NMDA receptors begin to express at synaptic sites even at an early stage of development (Fu et al. 2005).

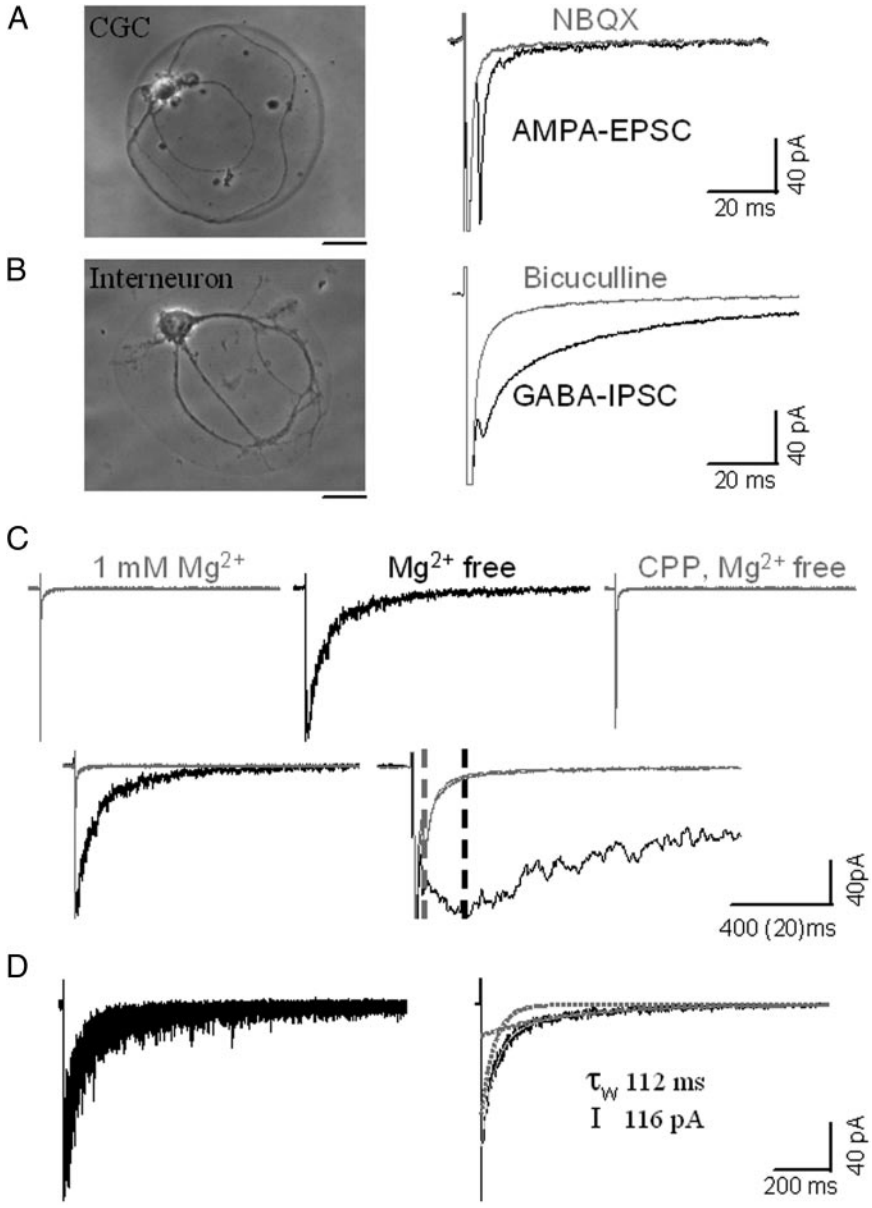

FIG. 1. Autaptic currents recorded from solitary cerebellar neurons. *A*, *left*: phase-contrast microphotograph illustrates an example of a solitary cerebellar granule neuron (CGC) in microisland. *Right*: stimulation of this neuron with a brief depolarization (from −70 to +10 mV for 0.5 ms) elicited a large autaptic current (*black trace*), which was blocked by 5 μM 2,3-dihydro-6-nitro-7-sulfamoyl-benzo(F)quinoxaline (NBQX, *gray trace*). *B*, *left*: phase-contrast microphotograph illustrates an example of a solitary cerebellar interneuron in microisland. *Right*: autaptic current (*black trace*) recorded from this cell was blocked by 25 μM bicuculline (*gray trace*). *C*: autaptic excitatory postsynaptic currents (EPSCs) recorded from an 8 days in vitro (DIV8) solitary CGC from +/+ mice. *Top left*: *gray trace* illustrated the EPSC recorded in the presence of 1 mM extracellular Mg^{2+}. *Top middle*: when Mg^{2+} was removed from the extracellular solution, the current became larger and long-lasting (*black trace*). *Top right*: EPSC recorded from the same cell in Mg^{2+}-free solution and in the presence of 10 μM 3-[(±)-2-carboxypiperazin-4-yl]-propyl-1-phosphonic acid (CPP, *gray trace*). *Bottom*: *3 traces* on the *top* are shown overlapped with 2 distinct timescales. Dashed lines mark the peaks of α-amino-3-hydroxy-5-methyl-4-isoxazolepropionic acid (AMPA)-EPSCs (gray line) and *N*-methyl-D-aspartate (NMDA)-EPSCs (black line). *D*, *left*: superimposed image shows 10 consecutive NMDA-EPSCs recorded in the absence of Mg^{2+} from the same neuron in *C*. *Right*: average of the currents on the *left* (*black trace*) is shown with double-exponential curves (dashed lines) and the indications of weighted decay time constant (τ_w) as well as peak amplitude (*I*) from the fitting of this current (*gray trace*).

The NMDA-receptor–mediated charge transfer (Q) during synaptic activation, the product of amplitude and decay time of the NMDA-EPSC, was compared between different experimental groups (Table 1). NMDA-EPSC peak amplitude was dominant in determining the increase in Q with development for all groups. In NR2A−/− cells, Q was significantly smaller at DIV8–9, but it increased with time in vitro, becoming similar to the value measured in +/+ cells at DIV12–13. With respect to the NR2C−/− group, Q at DIV8–9 was similar to that for cells from the +/+ group, although it exhibited a noticeable increase with age, which was significantly larger than that of other genotypes at DIV12–13 arising from its substantially larger peak amplitude.

The decay time constant and peak amplitude of AMPA-EPSCs are summarized in Table 1. AMPA-EPSC peak amplitudes increased from DIV8–9 to DIV12–13, similarly to that observed for NMDA-EPSCs, with no differences between different genotypes. In contrast, the decay times showed no differences between genotypes or between age groups. The parallel developmental increase of the AMPA-EPSC and NMDA-EPSC amplitudes suggested presynaptic changes with age in vitro (see following text); therefore we compared the NMDA to AMPA peak amplitude ratios between genotypes (Table 1). Although no significant developmental difference was observed in this ratio for all genotypes, it was notably smaller in NR2A−/− cells at all time points examined, suggesting that loss of NR2A subunit was not compensated. In contrast, the NMDA to AMPA peak amplitude ratio became significantly larger in NR2C−/− cells at DIV12–13, implying that the expression of the NR2C subunit plays a role in selectively reducing the amplitude of the NMDA current.

Changes of quantal parameters of NMDA-EPSCs in developing solitary CGCs

To investigate whether the observed differences of autaptic NMDA-EPSCs between genotypes were the result of presynaptic changes involving synapse formation and/or release prob-

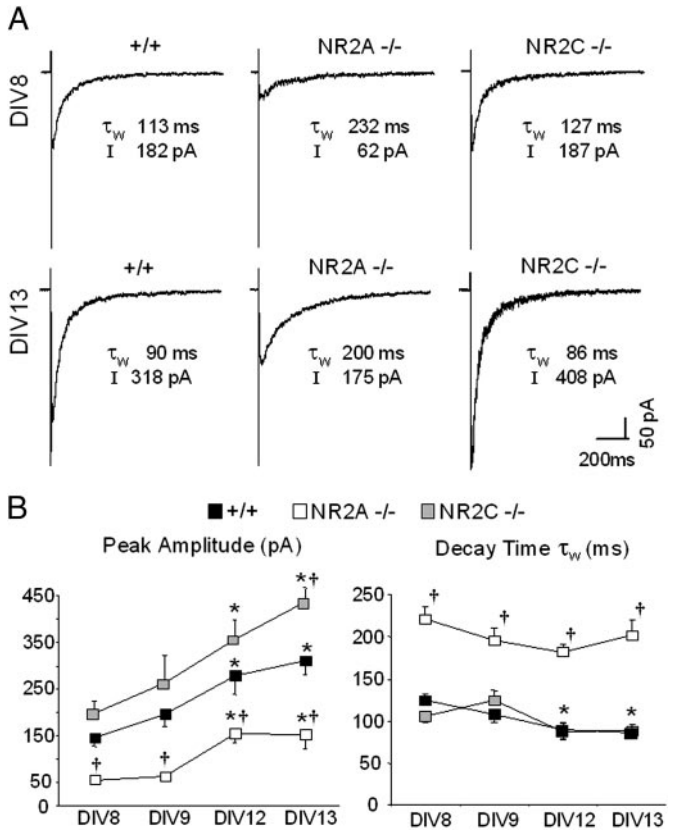

FIG. 2. Developmental changes of autaptic NMDA-EPSCs in solitary CGCs from +/+, NR2A−/−, and NR2C−/− mice. *A*: representative averages of autaptic NMDA-EPSCs recorded at DIV8 (*top traces*) and DIV13 (*bottom traces*) from +/+ (*left*), NR2A−/− (*middle*), and NR2C−/− (*right*) solitary CGCs with indications of their corresponding decay time constant (τ_w) and peak amplitude (*I*). *B*: summary of the analysis of progressive developmental changes of peak amplitude (*left*) and decay time (*right*) of autaptic NMDA-EPSCs in solitary CGCs from +/+ (■), NR2A−/− (□), and NR2C−/− (▩) mice at 4 distinct ages in vitro. Data derived from ≥10 cells in each experimental group from ≥3 different culture preparations. †, significant difference in comparison to +/+ at the same age ($P < 0.01$); *, significant difference in comparison to DIV8 within same genotype ($P < 0.01$). Because the decay times for +/+ and NR2C−/− overlap at DIV12 and DIV13, * in the *right graph* indicates significant difference to DIV8 within genotype for both strains.

ability related to the presence of specific NR2 subunit of NMDA receptors, we examined the quantal size and quantal content of autaptic NMDA-EPSCs recorded from +/+, NR2A−/−, and NR2C−/− solitary CGCs in two age groups: DIV8–9 and DIV12–13.

We used two different methods to estimate the quantal size, the amplitude of spontaneous miniature synaptic currents, and the amplitude of the evoked synaptic currents recorded with an extracellular calcium concentration sufficiently reduced to produce failures. Because the solitary neuron was voltage clamped at −70 mV, we directly recorded the spontaneous NMDA-EPSCs without adding TTX to block the action potential, and considered them to be the spontaneous miniature NMDA-EPSCs. In three solitary +/+ cells at DIV9, application of TTX (0.5 μM) did not change the amplitude and frequency of occurrence of these currents, similarly to that reported for hippocampal neurons (Gompert et al. 2000). Examples of miniature NMDA-EPSCs recorded from +/+ and NR2C−/− solitary neurons at DIV13 are shown in Fig. 3*A*. The high-input resistance of CGCs allowed us to visualize overlapping channel currents during these events (Clark et al. 1997). Reducing the extracellular calcium concentration decreases presynaptic release probability. This reduced the amplitudes of NMDA-EPSCs and increased the failure rate. A failure was seen as a current trace where no NMDA channel openings were observed after the action potential. As illustrated in Fig. 3*B*, the evoked autaptic current recorded from a +/+ solitary neuron at DIV8 displayed a failure rate of 70% with 0.25 mM extracellular calcium. In another +/+ solitary neuron at DIV13, we had to decrease the calcium level to 0.1 mM to reach a comparable failure rate. We measured the averaged amplitude of the successes and compared it with that of spontaneous miniature NMDA-EPSCs. As shown in Fig. 3*C*, the average spontaneous NMDA-EPSCs and the average evoked response (not counting failures) recorded under 0.25 mM calcium from the same +/+ solitary CGCs at DIV8 were quite similar in both the peak amplitude and decay time, suggesting both methods could be used to estimate the quantal size.

A summary of the data obtained from these two distinct procedures is reported in Table 2. Although we did not use the NMDA-EPSCs failures to assess quantal sizes for NR2A−/− neurons at DIV8–9 and NR2C−/− neurons at DIV12–13, we used the miniature spontaneous NMDA-EPSCs to compare quantal sizes among all groups. Our results show that the quantal sizes were not significantly different between genotypes at DIV8–9, but at DIV12–13 they were significantly smaller in the NR2A−/− group and larger in NR2C−/− group compared with the +/+ group (Table 2). Therefore the decreased autaptic NMDA-EPSC peak amplitudes in NR2A−/− neurons and the increased autaptic NMDA-EPSC peak amplitudes in NR2C−/− neurons at later developmental ages are apparently the result of changes in the elementary unit of synaptic transmission with the expression of specific NR2 subunit in solitary CGCs.

We estimated the quantal content of autapses at developing solitary CGCs from each genotype by dividing the average NMDA-EPSCs by the average quantal size obtained from the spontaneous miniature currents in each group. As reported in Table 2, the quantal content increased significantly from DIV8–9 to DIV12–13 for all three genotypes. In addition, except for the autapses in the NR2A−/− group at DIV8–9, whose quantal content was considerably smaller than that in the +/+ group, there were no other differences between genotypes at each age evaluated. Taken together, the increased quantal content might explain the increased NMDA-EPSC peak amplitude with development for all genotypes. It can also explain why the peak amplitude for autaptic NMDA-EPSCs in NR2A−/− neurons at DIV8–9 was smaller than that in +/+ neurons, although there was no quantal size difference between these two genotypes.

As described before, the average peak amplitude of NMDA-EPSCs recorded from the same cells was quite stable over time, although with noticeable individual variations. When we compared the variability of individual NMDA-EPSCs between ages, we found that, for all three genotypes, the coefficients of variation of peak amplitudes at DIV8–9 were significantly bigger (smaller $1/CV^2$, Table 2) than that at DIV12–13, indicating decreased NMDA-EPSC variability with development. This further supported changes in quantal content that could be attributable to increased release probability or in the number of

TABLE 1. *Summary of additional parameters characterizing autaptic EPSCs in cerebellar granule neurons*

	+/+		NR2A−/−		NR2C−/−	
Parameter	DIV8–9	DIV12–13	DIV8–9	DIV12–13	DIV8–9	DIV12–13
NMDA-EPSC charge transfer, pC	18 ± 2 (n = 75)	28 ± 3* (n = 58)	12 ± 1† (n = 35)	32 ± 5* (n = 23)	23 ± 3 (n = 31)	44 ± 5*† (n = 49)
AMPA-EPSCs						
Decay time, ms	5.1 ± 0.5 (n = 15)	5.5 ± 0.3 (n = 30)	5.2 ± 0.4 (n = 10)	5.6 ± 0.4 (n = 8)	5.5 ± 0.4 (n = 23)	5.7 ± 0.4 (n = 25)
Peak amplitude, pA	114 ± 21 (n = 15)	177 ± 15* (n = 30)	80 ± 9 (n = 10)	175 ± 42* (n = 8)	122 ± 13 (n = 23)	180 ± 16* (n = 25)
NMDA/AMPA ratio	1.5 ± 0.2 (n = 15)	1.8 ± 0.2 (n = 30)	0.8 ± 0.2† (n = 10)	0.9 ± 0.1† (n = 8)	2.1 ± 0.2 (n = 23)	2.7 ± 0.3† (n = 25)

Values are means ± SE. Quantification of parameters of synaptic currents is described in the text. *$P \leq 0.01$ vs. DIV8–9 within genotype. †$P < 0.05$ vs. +/+ at the same days in vitro (DIV).

release sites. Therefore we measured the ratio of paired-pulse responses for AMPA-EPSCs separated by 50 ms and found that it was not significantly different with age in culture (Table 2). Finally, we directly assessed the synaptic sites with immunostaining for the presynaptic proteins Synapsin and Bassoon (Fig. 4). The increased number of positive puncta with age in vitro suggests that the increase quantal content is probably the consequence of an increase in the number of release sites.

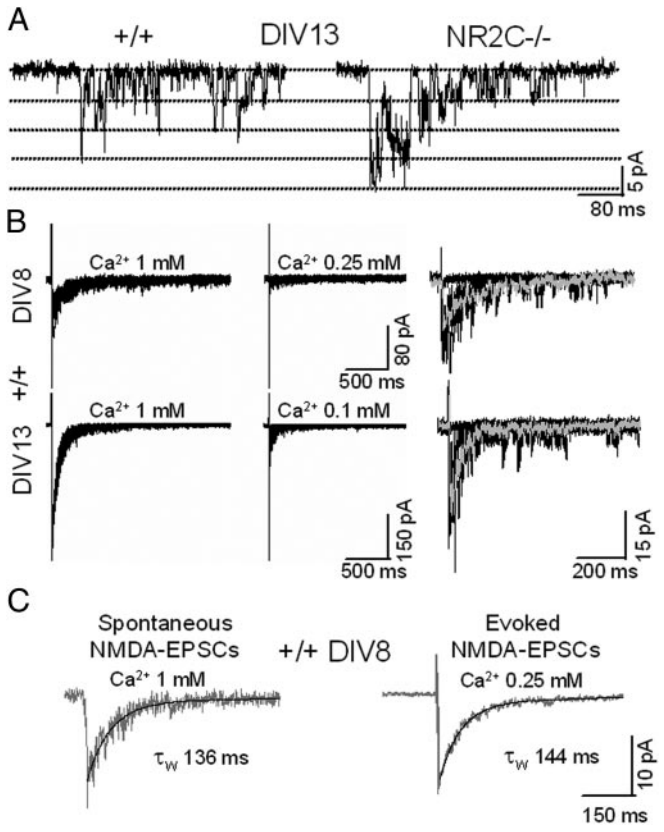

FIG. 3. Comparison of spontaneous and evoked NMDA-EPSCs in solitary CGCs. *A*: representative recordings of spontaneous NMDA-EPSCs recorded from +/+ (*left*) and NR2C−/− (*right*) solitary CGCs at DIV13. *B*: examples of evoked NMDA-EPSCs from one DIV8 +/+ solitary CGC (*top traces*) and one DIV13 +/+ solitary CGC (*bottom traces*) recorded in different extracellular Ca^{2+} concentration. *Right column*: corresponding expanded traces from the *middle*. *Gray traces*: averages of nonfailure currents for each cell under reduced extracellular Ca^{2+}. *C*: average of 10 spontaneous NMDA-EPSCs (*left*) is compared with the average of 10 evoked NMDA-EPSCs under 0.25 mM extracellular Ca^{2+} (*right*) from the same DIV8 +/+ solitary CGC together with their respective decay times.

Synaptic and extrasynaptic distribution of NMDA receptors in solitary CGCs from different genotypes

We measured the expression of functional NMDA receptors in developing solitary CGCs from +/+, NR2A−/−, and NR2C−/− mice with application of a saturating dose of NMDA (200 μM) in the absence of calcium to prevent calcium-mediated inactivation. Whole cell NMDA currents represent the contribution of both synaptic and extrasynaptic receptors. We then took advantage of MK-801, a specific NMDA-receptor open-channel blocker, to study the portion of NMDA receptors selectively expressed at extrasynaptic sites (Rosenmund et al. 1993).

As illustrated in Fig. 5*A*, after applying NMDA to measure the whole cell NMDA current, autaptic EPSCs were repeatedly evoked in the presence of MK-801 (5 μM) until no significant NMDA-EPSCs could be observed. Because the binding of MK-801 to NMDA channels is practically irreversible in the absence of depolarization, the portion of extrasynaptic NMDA receptors can be derived from the ratio of whole cell current elicited by NMDA after and before MK-801 blockade. Then, the portion of synaptic NMDA receptors could be calculated from the percentage of the current blocked by MK-801.

The summary of NMDA current density and the portion of synaptic receptors are reported in Fig. 5*B*. In contrast with what was reported for mass cerebellar granule cell cultures (Fu et al. 2005), the current density was significantly increased from DIV8–9 to DIV12–13 for +/+ and NR2C−/− cells, but not for NR2A−/− cells. In addition, compared with +/+ neurons, significantly smaller current density was observed in NR2A−/− cells at each age group and significantly larger current density was observed in NR2C−/− neurons at DIV12–13. The data from MK-801 blockade experiments did not show a significant increase in the percentage of synaptic NMDA receptors with development for any genotype. Taken together, for +/+ and NR2C−/− cells, the increased current density and maintained synaptic portion with development parallel the increase of NMDA-EPSCs observed (Fig. 2). However, for NR2A−/− cells, there was no significant change of either current density or their distribution at synaptic sites estimated using MK-801 blockade, which suggested similar NMDA-EPSCs between ages in vitro. This was not consistent with the

TABLE 2. *Quantal parameters in solitary CGCs from different genotypes*

	+/+		NR2A−/−		NR2C−/−	
Parameter	DIV8–9	DIV12–13	DIV8–9	DIV12–13	DIV8–9	DIV12–13
Quantal size, pA						
Mini	24 ± 1 ($n = 10$)	27 ± 1 ($n = 13$)	20 ± 1 ($n = 4$)	22 ± 1† ($n = 6$)	27 ± 2 ($n = 9$)	37 ± 3*† ($n = 6$)
Low Ca^{2+}	21 ± 1 ($n = 13$)	25 ± 2 ($n = 9$)	ND	24 ± 2 ($n = 14$)	27 ± 3 ($n = 4$)	ND
Quantal content	7.1 ± 0.7 ($n = 78$)	11.1 ± 0.9* ($n = 64$)	3.0 ± 0.3† ($n = 36$)	8.4 ± 1.1* ($n = 24$)	7.8 ± 0.9 ($n = 32$)	11.3 ± 0.7* ($n = 54$)
I/CV^2	37 ± 5 ($n = 76$)	73 ± 13* ($n = 64$)	45 ± 4 ($n = 36$)	65 ± 2* ($n = 23$)	64 ± 3 ($n = 32$)	80 ± 2* ($n = 54$)
Paired-pulse ratio	0.89 ± 0.05 ($n = 8$)	0.90 ± 0.12 ($n = 3$)	ND	ND	1.09 ± 0.07 ($n = 6$)	0.93 ± 0.07 ($n = 13$)

Values are means ± SE. *$P \leq 0.01$ vs. DIV8–9 within genotype. †$P < 0.01$ vs. +/+ at the same days in vitro (DIV). ND, not determined; Mini, spontaneous miniature NMDA-EPSCs; CV, coefficient of variation for NMDA-EPSC peak amplitudes. Quantification of quantal parameters is described in the text. Paired-pulse ratio derives from the mean of the second peak divided by the mean of the first in the average AMPA-EPSCs separated by 50 ms.

developmentally increased NMDA-EPSCs observed in NR2A−/− cells (Fig. 2). Therefore we also compared the peak amplitude ratio of maximal synaptic current to whole cell current (Fig. 5*B*, *right*) to independently estimate the synaptic receptors portion with development. We found that similarly to what was observed with MK-801 blockade, this ratio was not

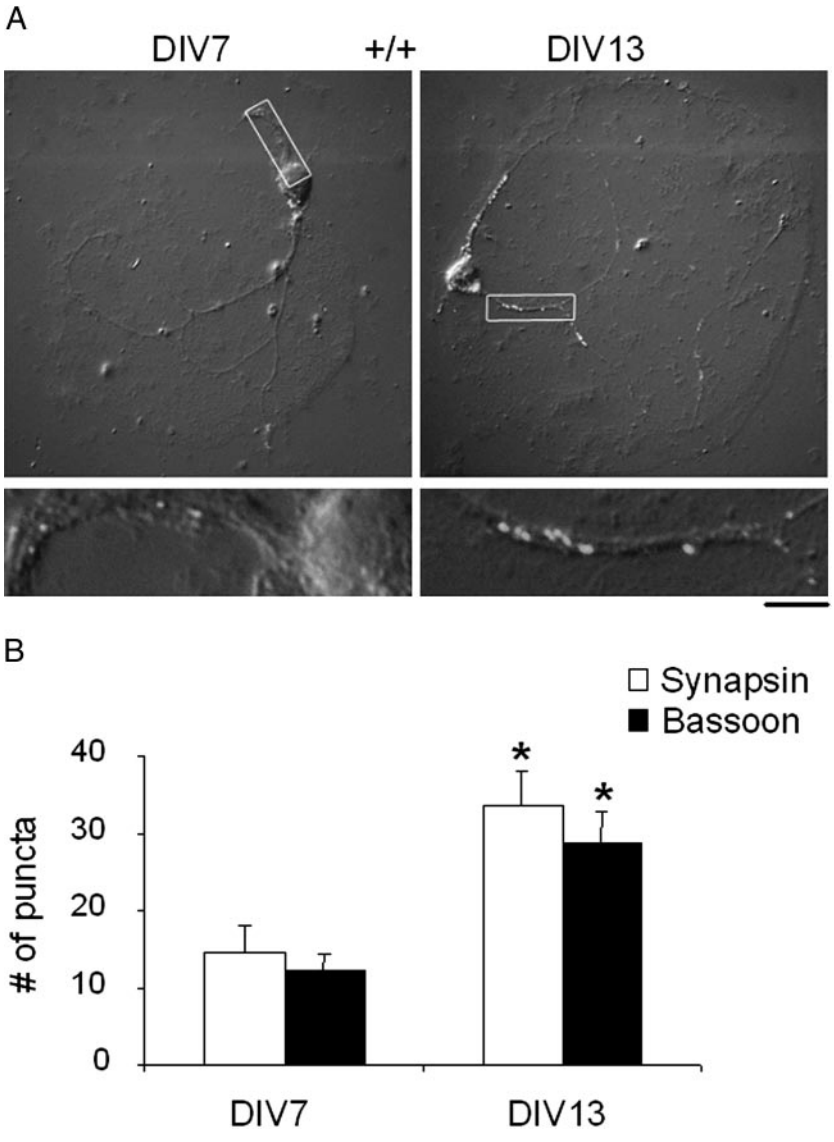

FIG. 4. Developmental changes in immunostaining of synaptic proteins in solitary CGCs from +/+ mice. *A*: examples of +/+ solitary CGCs in microislands at DIV7 (*left*) and DIV13 (*right*) labeled for the presynaptic protein Bassoon using green fluorescently tagged antibodies (Alexa 488). Images are shown overlapped with the matching Nomarski differential interference contrast (DIC) image. Region of the image highlighted by a dashed white box was reimaged with higher-resolution lens and shown magnified below in each panel. Exposure and threshold for both images are identical, allowing for a qualitative appreciation of the increase in synapses with age in vitro. Scale bar is 10 and 2.2 μm for the *insets*. *B*: summary of the number of positive boutons per cell (# puncta) from immunohistochemical investigations using synapsin and bassoon as markers of synapses at different ages in culture. *, significant difference in comparison to DIV7 ($P < 0.01$).

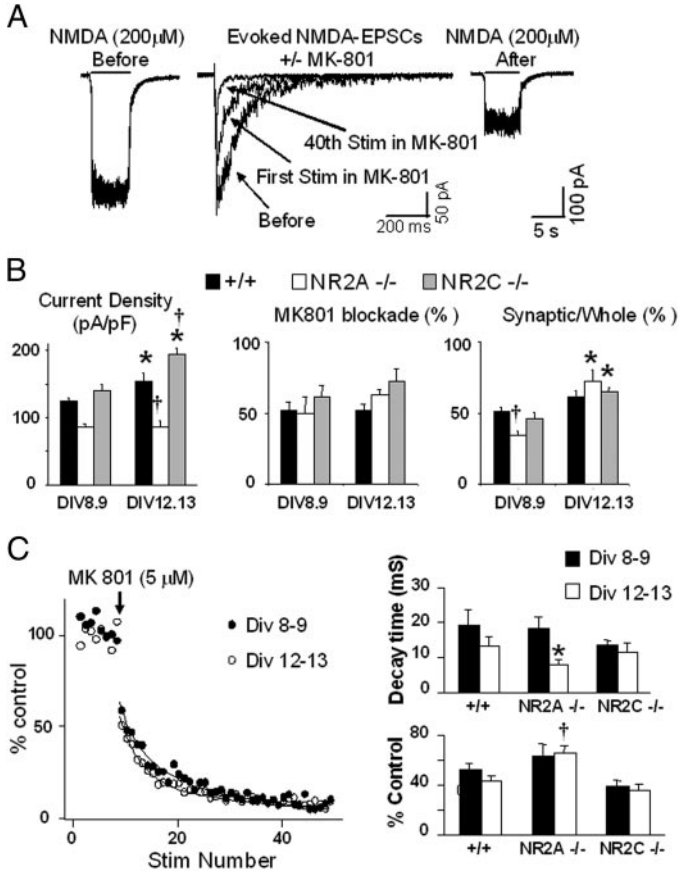

FIG. 5. NMDA current density and the relative proportion of synaptic NMDA receptor in +/+, NR2A−/−, and NR2C−/− CGCs with age in vitro. *A*: illustration of the experimental procedure used to determine the NMDA current density and the relative proportion of synaptic NMDA receptors in solitary CGCs at DIV9. Whole cell application of 200 μM NMDA was followed by progressive stimulation of the autapses in the presence of MK-801 (5 μM) that gradually decreased the current until its almost complete disappearance resulting from blockade of synaptic receptors. Stimulation frequency was 0.2 Hz. Sequential application of 200 μM NMDA activated a current generated from extrasynaptic receptors. *B*: summary results of NMDA current density measured in different genotypes from whole cell NMDA application shown in *A* (*right*), the percentage of the current blocked by MK-801 (*middle*), and the ratio of the maximal autaptic NMDA-EPSC to the NMDA whole cell current (Synaptic/Whole) in each cell studied (*right*). Data derived from ≥17 cells in each group for current density experiments and Synaptic/Whole experiments and ≥7 cells in each group for MK-801 blockade experiment from ≥2 culture preparations. *, significant difference in comparison to DIV8–9 within same genotype ($P < 0.01$); †, significant difference in comparison to +/+ at the same age ($P < 0.01$). *C*: illustration of the initial extent and the time course of the progressive blockade of MK-801 in +/+ solitary CGCs in the 2 age groups (*left*). Summary of the weighted decay time derived from the double-exponential fitting of the rate of decline in the presence of MK-801 (*right: top*, decay time) and the initial NMDA-EPSCs blockade (*right: bottom*, % control) in all genotypes considered. Data derived from ≥9 cells in each experimental group. *, significant difference in comparison to DIV8–9 within same genotype ($P < 0.01$); †, significant difference in comparison to +/+ at the same age ($P < 0.01$).

significantly different in +/+ group between ages, but increased remarkably in both NR2A−/− and NR2C−/− groups from DIV8–9 to DIV12–13, implying a larger portion of NMDA receptors located at synaptic sites in these two genotypes with development. In combination with the current density, this result agrees with the increased NMDA-EPSCs in NR2A−/− cells and perhaps provides a better assessment of the changes in proportion of synaptic receptors.

We then compared the extent of blockade by the NR2B selective blocker CP101,606 (10 μM) of the total whole cell NMDA responses and the extrasynaptic component in +/+ mice. The whole cell NMDA current was reduced 52 ± 4% by CP101,606 before synaptic MK-801 blockade and 60 ± 8% after in cells at DIV8–9. In contrast, the reduction was 34 ± 11% with CP101,606 before MK-801 application and 42 ± 3% after in cells at DIV12–13. The changes in CP101,606 reduction between synaptic and extrasynaptic receptors were not significant, but the changes with age in vitro were significant ($P < 0.05$).

We also compared the rate of decline and the extent of initial MK-801 blockade of the NMDA-EPSCs in the presence of MK-801 for different genotypes (Fig. 5*C*). We saw a trend in faster decline with age in vitro, although this was significant only in the NR2A−/− group. In addition, in NR2A−/− group at DIV12–13, the initial MK blockade was also significantly smaller compared with the +/+ group. These parameters were previously used to assess the changes in vitro of release probability with development (Chavis et al. 2001). However, because postsynaptic NMDA receptors have distinct subunit composition in the different genotypes, the distinct channel open probability will also influence the rate and initial MK blockade. In fact, the significantly reduced rate of decline and initial MK blockade with NR2A−/− at DIV13 may suggest that both changes in release and postsynaptic channel open probability were taking place in this group.

Subunit composition of synaptic NMDA receptors in developing solitary CGCs

A number of pharmacological agents have been used to distinguish NMDA receptor subtypes. CP101,606 has been reported to be a selective NR1/NR2B subunit antagonist with less potent actions on NR1/NR2A/NR2B heteromers (Hatton and Paoletti 2005; Mott et al. 1998). In contrast, Conantokin G has been shown to be able to selectively block NR1/NR2B and NR1/NR2A/NR2B triheteromers (Barton et al. 2004). In addition, Conantokin G at high concentrations (about 50 μM) has also been shown to partially block NR1/NR2A receptors when the exon 5 containing NR1 splice variant is present (Klein et al. 2001; Ragnarsson et al. 2006). Here, we used Conantokin G at two different concentrations (0.6 and 1.2 μM) and 10 μM CP101,606 to investigate the presence of synaptic NMDA receptor subtypes in +/+ and NR2A−/− solitary CGCs with development.

Sample traces of NMDA-EPSCs in cells at DIV8 from both genotypes recorded in the presence or the absence of 0.6 μM Conantokin G and 10 μM CP101,606 are illustrated in Fig. 6. As summarized in Fig. 6*B*, *left*, both compounds decreased the peak amplitude of NMDA-EPSCs. Their effects were significantly stronger in NR2A−/− than in +/+ CGCs at all time points examined. This supported the expression of NR2B subunit containing NMDA receptors at synaptic sites in both genotypes and also implied that the proportions of NR1/NR2B receptors were always smaller in +/+ than in NR2A−/− solitary CGCs. We also observed that, for both genotypes, 10 μM CP101,606 showed significantly reduced effects with development. In addition, compared with 1.2 μM Conantokin G, 10 μM CP101,606 displayed a similar effect at DIV8 and a considerably smaller effect at DIV13, which suggests changes

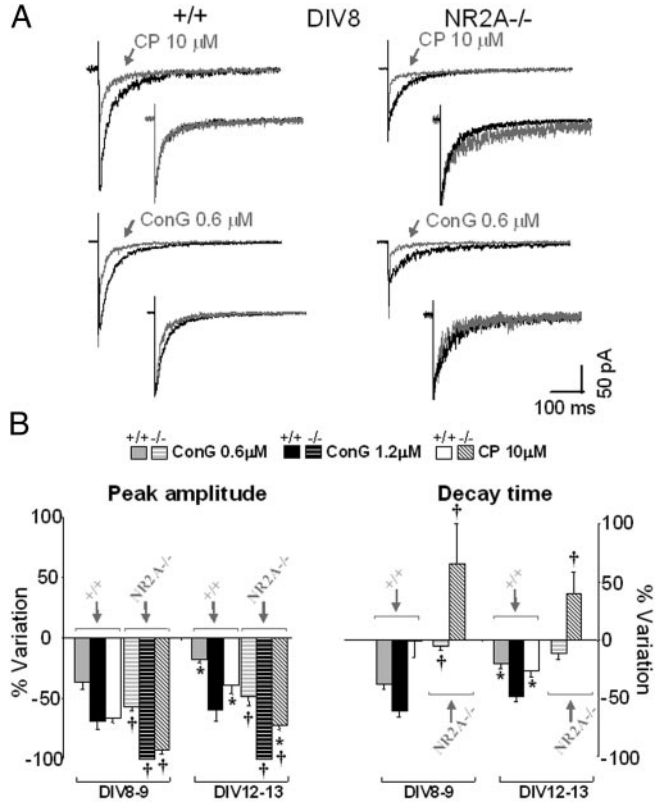

FIG. 6. Distinct actions of Conantokin G (ConG) and CP101,606 (CP) on the peak amplitude and decay time of autaptic NMDA-EPSCs in solitary CGCs from +/+ and NR2A−/− mice. *A*: representative averages of autaptic NMDA-EPSCs recorded before (*black traces*) and during (*gray traces*) local application of ConG or CP as indicated in solitary CGCs at DIV8 from +/+ mice (*left column*) and NR2A−/− mice (*right column*). Current peaks in each pair of traces are normalized and shown *below* and to the *right*. *B*: summary of the percentage variation from control in 0.6 or 1.2 mM ConG and 10 mM CP on the peak amplitude (*left*) and decay time (*right*) of autaptic NMDA-EPSCs recorded from solitary CGCs at different days in vitro and in distinct genotypes. Data derived from ≥7 cells in each experimental group from 2 culture preparations. *, significant difference in comparison to DIV8 within same genotype ($P < 0.01$); †, significant difference in comparison to +/+ at the same age ($P < 0.01$).

in receptor composition of synaptic NMDA receptors with age in culture in both +/+ and NR2A−/− mice. Thus the changes in the antagonism of Conantokin G and CP101,606 with age in vitro demonstrated the changes in NMDA receptor subtypes. This perhaps relates to the presence of distinct heterotrimeric Conantokin G–sensitive receptors in both genotypes.

We also examined the effects of Conantokin G and CP101,606 on the decay kinetics of NMDA-EPSCs. Because 1.2 μM Conantokin G almost completely blocked NMDA-EPSCs in NR2A−/− groups, it was impossible to measure kinetic changes. We therefore selected a lower Conantokin G concentration (0.6 μM) to allow a comparison with the effect of CP101,606. As shown in Fig. 6*B*, *right*, in the +/+ group at DIV8, CP101,606 failed to alter NMDA-EPSC decay times, whereas Conantokin G remarkably sped up the NMDA-EPSCs at both concentrations tested. Most likely, this differential effect is a result of the stronger blockade of synaptic NR1/NR2A/NR2B receptors by Conantokin G compared with that by CP101,606. An alternative explanation for faster NMDA-EPSC decay in +/+ cells with Conantokin G is a direct change in the deactivation kinetic of NR1/NR2B receptor with this compound. This, however, is ruled out by lack of the effect of 0.6 μM Conantokin G on NMDA-EPSC decay in the NR2A−/− group. However, our interpretation of the differential effects of Conantokin G and CP101,606 needs to consider the surprisingly slower decay time of the small residual NMDA-EPSCs recorded in the presence of CP101,606 in NR2A−/− CGCs at both age groups, as discussed later. In the +/+ group at DIV13, the NMDA-EPSC decay reduction by CP101,606 was larger than that seen at DIV8, although significantly smaller than that seen with 1.2 mM Conantokin G. This further supports the hypothesis of a developmental change in the relative proportion of NR1/NR2A, NR1/NR2B, and triheteromeric NR1/NR2A/NR2B receptors.

Although the decay of NMDA-EPSCs was consistently slower in NR2A−/− than that in +/+ neurons, it was remarkably faster than in slice preparations. One possibility is that neurons in microislands have a high content of exon 5–containing NR1 subunits, which has been reported to speed up the deactivation of NR1/NR2B channel (Rumbaugh et al. 2000). Because this effect is shared with spermine (Rumbaugh et al. 2000), we investigated spermine action on NMDA-EPSCs. In four cells from NR2A−/− mice at DIV9, spermine (300 mM) failed to affect the amplitude of NMDA-EPSCs, but it changed the τ_w of decay from 231 ± 9 to 159 ± 12 ms, which suggests the consistent presence of NR1 receptors with the exon 5 cassette in solitary neurons.

NMDA receptors containing NR2C subunit exhibit a lower sensitivity to Mg^{2+} and participate in synaptic transmission in the adult cerebellum (for review see Cull-Candy and Leszkiewicz 2004). To test whether NR1/NR2C receptors also contribute to autaptic NMDA-EPSCs, we compared the dose-dependent Mg^{2+} inhibition of NMDA-EPSCs and whole cell current from +/+ and NR2C−/− solitary CGCs. As illustrated in Fig. 7, at early developmental ages, there were similar reductions of synaptic and whole cell NMDA currents with increased concentration of Mg^{2+} between two genotypes. However, at later days in vitro, we observed significant reductions in Mg^{2+} sensitivity at several concentrations in cells from the +/+ group (Fig. 7*B*), resulting in a higher IC_{50} for Mg^{2+} blockade. The change in Mg^{2+} sensitivity was not observed in cells from NR2C−/− groups.

It was previously reported that coexpression of the NR3A subunit with NR1 and other NR2 subunits may also decrease the Mg^{2+} sensitivity (Sasaki et al. 2002). However, these channels could also be inhibited by 100 μM D-serine (Chatterton et al. 2002). In five CGCs from +/+ mice at DIV13, we did not observe changes in the NMDA-EPSCs with increased extracellular D-serine concentration (from 10 μM to 100 μM), suggesting that it is unlikely that this subunit participates to any significant degree to the changes in the Mg^{2+} sensitivity of the NMDA-EPSCs.

Western blot analysis of the expression of distinct NMDA receptor subunit in the cerebellum of +/+, NR2A−/−, and NR2C−/− mice

To quantitatively assess the expression of distinct NMDA receptor subunit, Western blot analysis is a very reliable quantitative approach. This quantitative analysis of subunit expression cannot be performed in solitary neurons because of the extremely small amount of protein in isolated cell. There-

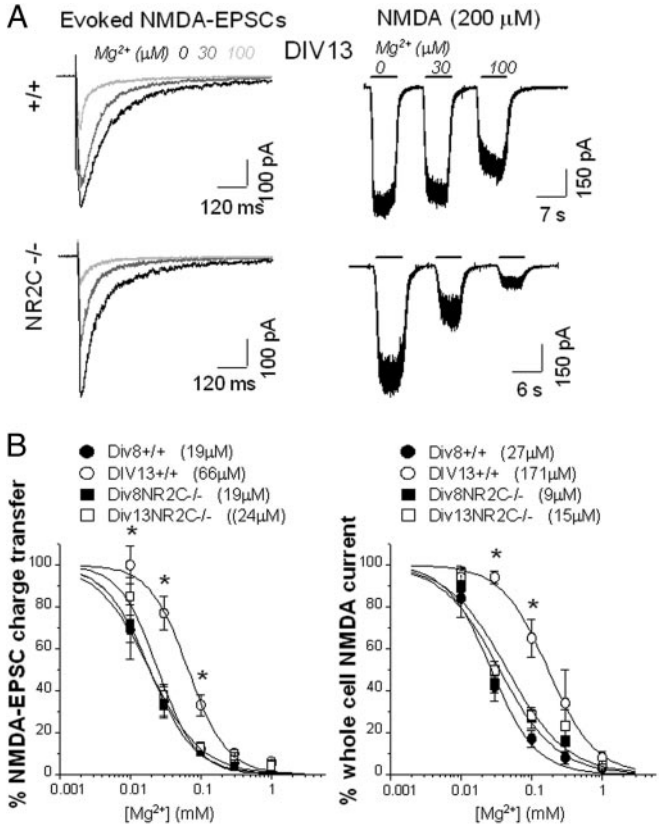

FIG. 7. Developmental changes of NMDA receptors' sensitivity to Mg^{2+} in +/+ and NR2C−/− solitary CGCs. *A*: examples of average autaptic NMDA-EPSCs (*left*) and whole cell NMDA currents (*right*) elicited in the same cell by local application of 200 μM NMDA in the presence of Mg^{2+} at different concentrations in solitary CGCs at DIV13 from +/+ and NR2C−/− mice as indicated. *B*: summary of the results obtained from experiments as those shown in *A*. Reduction of the average NMDA-EPSCs charge (*left*) and whole cell NMDA currents (*right*) with increasing extracellular Mg^{2+} were compared between 2 age groups (DIV8–9; DIV12–13) and 2 genotypes (+/+; NR2C−/−). Data derived from ≥12 cells in each experimental group from 3 culture preparations. IC_{50} values are shown in parentheses. *, significant difference in comparison to DIV8–9 wild-type ($P < 0.01$).

fore we performed Western blot analysis using the whole cerebellum from P21 mice of each genotype because this developmental age is loosely comparable to DIV14 autaptic culture. Previous studies reported the analysis of only NR2B subunit expression in NR2A−/− mice with Western blots (Takahashi et al. 1996). Our data extended these results by including the expression of NR1, NR2A-D, and NR3A subunits in +/+, NR2A−/−, and NR2C−/− mice (Fig. 8). Although the comparison between cerebella in developing mice and solitary CGCs in culture can be considered only in relative terms, the in vivo changes in NMDA-receptor subunit expression with NR2A or NR2C subunit deletion are supportive of the electrophysiological results obtained from in vitro solitary neuron studies. As summarized in Fig. 8*B*, deletion of the NR2C subunit caused a significant reduction in the expression of NR1, NR2A, and NR2B subunits. NR2A subunit deletion did not alter the expression of NR2B subunit, as reported before (Takahashi et al. 1996), whereas the NR2C subunit decreased. The expression of both NR2D and NR3A subunits was also detected, although there were no differences among genotypes.

DISCUSSION

Using whole cell voltage-clamp recordings and immunohistochemical staining, we studied the developmental changes of autaptic excitatory synaptic transmission in solitary cerebellar granule cells with deletion of specific NR2 NMDA subunits. Significant changes were seen in the relative amplitudes of AMPA-receptor– and NMDA-receptor–mediated autaptic EPSCs and in the NMDA-EPSC decay kinetics in NR2A−/− and NR2C−/− CGCs compared with +/+. These results correlated well with the changes in the properties of excitatory synaptic transmission at cerebellar mossy fiber–granule cell synapses seen in vivo (Cathala et al. 2000). The developmental increase in peak amplitudes of autaptic NMDA-EPSCs in all genotypes is related to the progressive increase in quantal content. This was supported by the developmental increase in the number of synaptic boutons in solitary +/+ CGCs (Fig. 4).

NR2A subunit deletion

In comparison to wild-type neurons, the deletion of NR2A subunits resulted in smaller peak amplitude of autaptic NMDA-EPSCs with reduced quantal size and quantal content. In addition, the NMDA to AMPA ratio almost halved compared with +/+ groups at all ages examined, indicating that the loss of NR2A-containing synaptic NMDA receptors was uncompensated. Interestingly, the charge transfer of NR2A−/− cells increased considerably with age and was even larger than that of +/+ cells at DIV12–13 (Table 1). Thus the smaller NMDA-EPSC amplitude was compensated by a slower decay time in the NR2A−/− group at a later age, maintaining synaptic charge transfer.

The decay times were slower in NR2A−/− cells than that in the other two genotypes at every age tested. As recombinant NR1/NR2A heterodimers have the fastest deactivation (Cull-Candy et al. 2001; for review see Cull-Candy and Leszkiewicz 2004), this suggests an abundance of this subunit from an early time after cell plating. Although a developmental decrease in the decay times of autaptic NMDA-EPSCs was observed in +/+ solitary CGCs, it was of lesser extent compared with that reported in high-density CGCs cultures (Fu et al. 2005) or in cerebellar slices (Cathala et al. 2000; Rumbaugh et al. 1999). Taken together, these results indicate that NR2A-subunit–containing NMDA receptors already existed at synaptic sites during the first week after cell plating and their contribution to synaptic currents increased only slightly with development. Most likely, NR2A subunits at synaptic sites are upregulated during development in CGCs growing in solitary confinement. The decay of autaptic NMDA-EPSCs in NR2A−/− cells in solitary confinement is faster than the deactivation of NMDA responses from recombinant receptors lacking the exon 5 cassette (Rumbaugh et al. 2000). This suggests the presence of an exon 5–cassette-containing NR1 subunit in solitary NR2A−/− cells, which was also shown by the speed-up of autaptic NMDA-EPSC decay by spermine.

Both CP101,606 and Conantokin G reduced NMDA-EPSCs in +/+ solitary CGCs at DIV8–9, but they showed decreased efficacy at later developmental ages. This supports the synaptic expression of NR1/NR2B heterodimers and suggests the increased incorporation of other NMDA-receptor subtypes at synaptic sites over development. In the group at DIV13, 1.2 μM Conantokin G had a significantly greater effect than 10

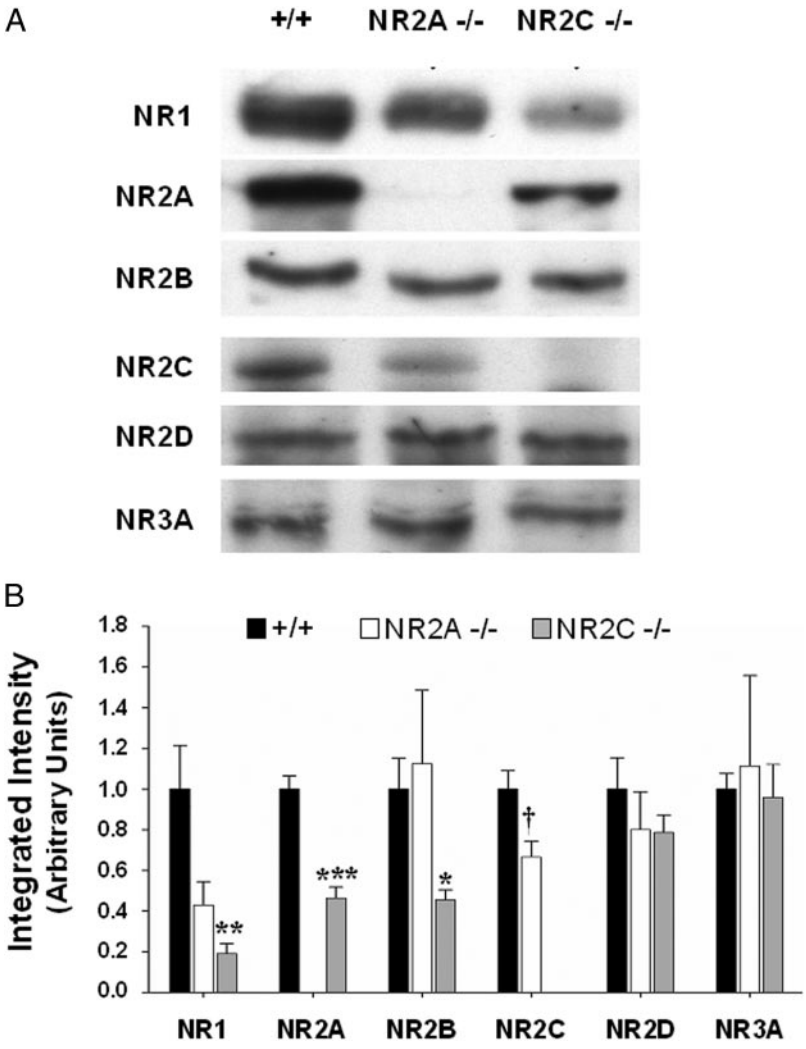

FIG. 8. Western blot analysis of the expression of distinct NMDA receptor subunit in the cerebellum of +/+, NR2A−/−, and NR2C−/− mice. Western blots were performed and quantified as described in METHODS. Expression of NMDA receptor subunit in the cerebellum of +/+, NR2A−/−, and NR2C−/− mice at p21 was detected by subunit-specific antibodies against NR1, NR2A-D, and NR3A subunits. *A*: representative Western blots. *B*: quantitative analysis of the relative amount of each NMDA receptor subunit in the cerebellum from +/+, NR2A−/−, or NR2C−/− mice by quantification of the integrated intensity of the immunoreactive bands in arbitrary units. Data derived from 9 +/+, 4 NR2A−/−, and 9 NR2C−/− mice from 2 separate litters. *, significant difference in comparison to +/+ (ANOVA, $P < 0.05$; Bonferroni, $P < 0.05$). **, significant difference in comparison to +/+ (ANOVA, $P < 0.005$; Bonferroni, $P < 0.005$). ***, significant difference in comparison to +/+ (ANOVA, $P < 0.001$; Bonferroni, $P < 0.001$). †, significant difference in comparison to +/+ (ANOVA, $P < 0.001$; Bonferroni, $P < 0.05$).

μM CP101,606, suggesting the increased contribution of NR1/NR2A/NR2B heterotrimeric receptors. The distinct antagonism of the two drugs at DIV12–13 was also maintained in the NR2A−/− group, leading to a possibility of the presence of Conantokin G–sensitive heterotrimeric receptors containing NR1, NR2B, and another NR2 subunit.

Further support for the existence of heterotrimeric receptors came from analysis of the effect of the NR2B antagonists on NMDA-EPSC decays. CP101,606 failed to alter NMDA-EPSCs decay times in +/+ solitary CGCs, similarly to what was reported for the parent compound, ifenprodil, on autaptic NMDA-EPSCs in microisland hippocampal cultures (Thomas et al. 2006). As suggested by these authors, this argues against separate populations of pure NR1/NR2A and NR1/NR2B receptors. Indeed Conantokin G, which was previously reported to antagonize both NR1/NR2B and NR1/NR2A/NR2B heterotrimeric receptors (Barton et al. 2004), made the decay of NMDA-EPSCs faster in +/+ but not in NR2A−/− CGCs. One concern for this interpretation is the slower decay time of the residual NMDA-EPSCs in NR2A−/− CGCs recorded with CP101,606. This slower component may counteract the changes in NMDA-EPSC decay expected from a smaller contribution of pure NR1/NR2B receptors when CP101,606 is present. We propose, however, that the contribution of this residual component to wild-type NMDA-EPSC is probably too small to significantly contribute to this effect. The origin of the slow down of the residual NMDA-EPSCs in NR2A−/− CGCs with CP101,606 must be further investigated. It could be the result of a direct effect on the deactivation kinetic of NR1/NR2B receptor, or of the intriguing possibility that NMDA receptors with much slower decay kinetics are expressed at synaptic sites in NR2A−/− solitary CGCs. These receptors could possibly contain the NR2D subunit.

NR2C subunit deletion

Deletion of the NR2C subunit in solitary CGCs had several effects on autaptic NMDA-EPSCs with age in vitro. The increase in NMDA-EPSC amplitude resulted in the increase of the charge transfer, compared with that of wild-type. The NMDA/AMPA ratio was also significantly greater in neurons from these mice at DIV12–13 compared with the other genotypes, suggesting a selective enhancement of the NMDA component of the excitatory current. The significant increase in the amplitude of spontaneous miniature NMDA-EPSCs in NR2C−/− solitary neurons compared with +/+ probably underlies these changes. As discussed in Ebralidze et al. (1996), this can be explained by several possibilities, including

compensatory changes in the expression of NR1 or NR2 subunits. Also, deleting NR2C subunits allows only receptors with NR2A subunits to be formed, resulting in a larger ensemble current because of the larger unitary conductance of NR1/NR2A versus NR1/NR2C channels. In addition, the shorter open time of currents from NR2C-containing channels (Farrant et al. 1994) could make the peak NMDA current smaller simply arising from nonsynchronous opening and closing. This can be clearly seen in Fig. 3*A*, where NR2C−/− CGCs showed significantly longer channel openings, suggesting that the single-channel properties are crucial in determining the quantal size. Further studies need to be performed to quantify this aspect.

We performed comparative immunoblotting of NMDA receptor subunits in cerebellar tissues derived from postnatal day 21 +/+, NR2A−/−, and NR2C−/− mice. Although the comparison of changes in NMDA-receptor subunit expression during development in vivo is difficult to relate to developmental in vitro in microisland cultures, it showed remarkable a decrease in NR1, NR2A, and NR2B subunit expression with the deletion of the NR2C subunit. However, because NMDA-EPSCs are larger in NR2C−/− than in +/+ CGCs (Ebralidze et al. 1996), the results of immunoblotting seem to suggest that the functional changes in NMDA-EPSCs are not a result of the subunits' overexpression. This supports the hypothesis of the NMDA channel property as the main determinant of the increase in NMDA-EPSCs in NR2C−/− mice. Indeed, the enhanced channel current resulting from NR2C subunit deletion may be the cause of a compensatory downregulation of subunit expression both in vivo and in isolated CGCs.

To further support the hypothesis that NR1/NR2C receptors also contribute to autaptic NMDA-EPSCs, we compared the Mg^{2+} sensitivity of NMDA receptors from +/+ and NR2C−/− solitary CGCs. The data illustrated in Fig. 7 strongly support the existence of NR2C-containing NMDA receptors in solitary CGCs characterized by lower Mg^{2+} sensitivity. One puzzling aspect of our data is that, in contrast to a report from cerebellar slices from NR2C−/− mice (Ebralize et al. 1996), deletion of the NR2C subunit failed to speed up the decay of autaptic NMDA-EPSCs. One possibility is that, although the expression of the NR2C subunit is sufficient to change the size of the current and Mg^{2+} sensitivity, it does not influence the decay. Interestingly, in cerebellar slices of +/+ mice, the decreased sensitivity to Mg^{2+} blockade precedes in development the slowing of the NMDA-EPSC decay (Cathala et al. 2000). Thus one can propose that different levels in the expression of the NR2C subunit may independently regulate Mg^{2+} sensitivity, the size of the synaptic current, and its decay. A slow decay of NMDA-EPSCs in cells kept in culture for longer times may provide the definite evidence for the increased incorporation of NR2C subunits, similar to what was observed in the slice preparation (Cathala et al. 2000). Different levels in the expression of the NR2C subunit in development can give rise to the occurrence of mixed populations of NR1/NR2C and NR1/NR2A/NR2C channels with distinct biophysical properties such as deactivation time and Mg^{2+} sensitivity. Our Western blot analysis shows a significant decrease of the NR2A subunit expression in cerebellum of NR2C−/− mice. These data may imply that reduction of the NR2A subunit is attributable to the loss of heterotrimeric NR1/NR2A/NR2C channels as a consequence of the NR2C subunit deletion.

In summary, we can observe developmental increases in the NR2C subunit expression in solitary granule neurons as reported in vivo. The enhanced NR2C expression together with the NR2A subunit upregulation as discussed above suggest that, in solitary cultures, there are factors that speed up the developmental progression of subunit expression compared with other in vitro models of cerebellar development (Audinat et al. 1994). The temporary exposure of the culture to 25 mM potassium (Vallano et al. 1996), combined with possibly enhanced synaptic activity in autaptic cultures, may be among these factors.

Synaptic and extrasynaptic NMDA receptors

Figure 5*A* reports the increase of NMDA current density with age in vitro for both +/+ and NR2C−/− but not for NR2A−/− neurons. These data contrast somewhat with the data in mass granule cell cultures (Fu et al. 2005), in which a progressive decline of current density was reported for both +/+ and NR2A−/− neurons. This is likely explained by differences in the synaptic inputs in these distinct model systems, perhaps related to the lack of inhibitory synaptic input in solitary CGCs. The proportion of NMDA receptors selectively expressed at extrasynaptic sites in solitary CGCs, as seen with MK-801 blockade, showed no significant differences among genotypes and ages studied. However, the maximal synaptic current to whole cell current ratio suggested a larger portion of NMDA receptors located at synaptic sites in both NR2A−/− and NR2C−/− groups at DIV12–13. This better mirrors the changes with genotype age in vitro in whole current density and NMDA-EPSC amplitude. The discrepancy between the two approaches is possibly explained by the fact that MK-801 blockade is more related to changes in the charge transfer of NMDA-EPSCs rather than the amplitude.

Using CP101,606, we estimated the proportion of NR1/NR2B receptors in the synaptic and extrasynaptic population in +/+ cells. This study revealed that composition of the two receptor pools does not differ and the changes taking place with development for synaptic receptors also happen for extrasynaptic ones. In cerebellar slices, however, extrasynaptic receptors selectively located on the cell body are more sensitive to the NR2B blocker (Rumbaugh et al. 1999). This is likely a result of the segregation of synapses in the glomeruli in slices (Palay and Chan-Palay 1974) but not in microisland cultures (Fig. 4).

Formation of excitatory autapses has been reported only from cultured neurons growing in solitary confinement, as opposed to inhibitory ones that can also be found in vivo (Bacci et al. 2005). Thus it is unlikely that CGCs make autaptic connections in vivo, making autapses of isolated CGCs nonphysiologic. Autapses in solitary CGCs, however, present remarkable similarity to excitatory synapses in cerebellar slices. This allows designing experiments to study excitatory synaptic transmission with high resolution, by taking advantage of the unique biophysical properties of granule neurons.

ACKNOWLEDGMENTS

We are grateful to Dr. Masayoshi Mishina for providing the NR2A−/− mice used in this study. We thank Dr. Kate Prybylowski for helpful discussions.

GRANTS

This work was supported by National Institute of Neurological Disorders and Stroke Grant NS-047700 to S. Vicini.

REFERENCES

Al-Hallaq RA, Jarabek BR, Fu Z, Vicini S, Wolfe BB, and Yasuda RP. Association of NR3A with the *N*-methyl-D-aspartate receptor NR1 and NR2 subunits. *Mol Pharmacol* 62: 1119–1127, 2002.

Audinat E, Lambolez B, Rossier J, and Crepel F. Activity-dependent regulation of *N*-methyl-D-aspartate receptor subunit expression in rat cerebellar granule cells. *Eur J Neurosci* 6: 1792–1800, 1994.

Bacci A, Huguenard JR, and Prince DA. Modulation of neocortical interneurons: extrinsic influences and exercises in self-control. *Trends Neurosci* 28: 602–610, 2005.

Barton ME, White HS, and Wilcox KS. The effect of CGX-1007 and CI-1041, novel NMDA receptor antagonists, on NMDA receptor-mediated EPSCs. *Epilepsy Res* 59: 13–24, 2004.

Bekkers JM and Stevens CF. Excitatory and inhibitory autaptic currents in isolated hippocampal neurons maintained in cell culture. *Proc Natl Acad Sci USA* 88: 7834–7838, 1991.

Cathala L, Misra C, and Cull-Candy S. Developmental profile of the changing properties of NMDA receptors at cerebellar mossy fiber-granule cell synapses. *J Neurosci* 20: 5899–5905, 2000.

Chatterton JE, Awobuluyi M, Premkumar LS, Takahashi H, Talantova M, Shin Y, Cui J, Tu S, Sevarino KA, Nakanishi N, Tong G, Lipton SA, and Zhang D. Excitatory glycine receptors containing the NR3 family of NMDA receptor subunits. *Nature* 415: 793–798, 2002.

Chavis P and Westbrook G. Integrins mediate functional pre- and postsynaptic maturation at a hippocampal synapse. *Nature* 411: 317–321, 2001.

Chen L, Chetkovich DM, Petralia RS, Sweeney NT, Kawasaki Y, Wenthold RJ, Bredt DS, and Nicoll RA. Stargazin regulates synaptic targeting of AMPA receptors by two distinct mechanisms. *Nature* 408: 936–943, 2000.

Clark BA, Farrant M, and Cull-Candy SG. A direct comparison of the single-channel properties of synaptic and extrasynaptic NMDA receptors. *J Neurosci* 17: 107–116, 1997.

Cull-Candy S, Brickley S, and Farrant M. NMDA receptor subunits: diversity, development and disease. *Curr Opin Neurobiol* 11: 327–335, 2001.

Cull-Candy SG and Leszkiewicz DN. Role of distinct NMDA receptor subtypes at central synapses. *Sci STKE* 2004: re16, 2004.

D'Angelo E, Rossi P, and Taglietti V. Different proportions of *N*-methyl-D-aspartate and non-*N*-methyl-D-aspartate receptor currents at the mossy fibre-granule cell synapse of developing rat cerebellum. *Neuroscience* 53: 121–130, 1993.

Dunah AW, Yasuda RP, Wang YH, Luo J, Davila-Garcia M, Gbadegesin M, Vicini S, and Wolfe BB. Regional and ontogenic expression of the NMDA receptor subunit NR2D protein in rat brain using a subunit-specific antibody. *J Neurochem* 67: 2335–2345, 1996.

Ebralidze AK, Rossi DJ, Tonegawa S, and Slater NT. Modification of NMDA receptor channels and synaptic transmission by targeted disruption of the NR2C gene. *J Neurosci* 16: 5014–5025, 1996.

Farrant M, Feldmeyer D, Takahashi T, and Cull-Candy SG. NMDA-receptor channel diversity in the developing cerebellum. *Nature* 368: 335–339, 1994.

Fu Z, Logan SM, and Vicini S. Deletion of the NR2A subunit prevents developmental changes of NMDA-mEPSCs in cultured mouse cerebellar granule neurons. *J Physiol* 563: 867–881, 2005.

Garthwaite J and Brodbelt AR. Glutamate as the principal mossy fibre transmitter in rat cerebellum: pharmacological evidence. *Eur J Neurosci* 2: 177–180, 1990.

Gomperts SN, Carroll R, Malenka RC, and Nicoll RA. Distinct roles for ionotropic and metabotropic glutamate receptors in the maturation of excitatory synapses. *J Neurosci* 20: 2229–2237, 2000.

Gomperts SN, Rao A, Craig AM, Malenka RC, and Nicoll RA. Postsynaptically silent synapses in single neuron cultures. *Neuron* 21: 1443–1451, 1998.

Hatton CJ and Paoletti P. Modulation of triheteromeric NMDA receptors by N-terminal domain ligands. *Neuron* 46: 261–274, 2005.

Kimura F, Otsu Y, and Tsumoto T. Presynaptically silent synapses: spontaneously active terminals without stimulus-evoked release demonstrated in cortical autapses. *J Neurophysiol* 77: 2805–2815, 1997.

Klein RC, Prorok M, Galdzicki Z, and Castellino FJ. The amino acid residue at sequence position 5 in the conantokin peptides partially governs subunit-selective antagonism of recombinant *N*-methyl-D-aspartate receptors. *J Biol Chem* 276: 26860–26867, 2001.

Kumura E, Kimura F, Taniguchi N, and Tsumoto T. Brain-derived neurotrophic factor blocks long-term depression in solitary neurones cultured from rat visual cortex. *J Physiol* 524: 195–204, 2000.

Li B, Chen N, Luo T, Otsu Y, Murphy TH, and Raymond LA. Differential regulation of synaptic and extra-synaptic NMDA receptors. *Nat Neurosci* 5: 833–834, 2002.

Luo J, Wang YH, Yasuda RP, Dunah A, and Wolfe BB. The majority of *N*-methyl-D-aspartate receptor complexes in adult rat cerebral cortex contain at least three different subunits. *Mol Pharmacol* 51: 79–86, 1997.

Mellor JR, Merlo D, Jones A, Wisden W, and Randall AD. Mouse cerebellar granule cell differentiation: electrical activity regulates the $GABA_A$ receptor a6 subunit gene. *J Neurosci* 18: 2822–2833, 1998.

Mennerick S and Zorumski CF. Glial contributions to excitatory neurotransmission in cultured hippocampal cells. *Nature* 368: 59–62, 1994.

Monyer H, Burnashev N, Laurie DJ, Sakmann B, and Seeburg PH. Developmental and regional expression in the rat brain and functional properties of four NMDA receptors. *Neuron* 12: 529–540, 1994.

Mott DD, Doherty JJ, Zhang S, Washburn MS, Fendley MJ, Lyuboslavsky P, Traynelis SF, and Dingledine R. Phenylethanolamines inhibit NMDA receptors by enhancing proton inhibition. *Nat Neurosci* 1: 659–667, 1998.

Murase K, Ryu PD, and Randic M. Excitatory and inhibitory amino acids and peptide-induced responses in acutely isolated rat spinal dorsal horn neurons. *Neurosci Lett* 103: 56–63, 1989.

Palay SL and Chan-Palay V. *Cerebellar Cortex: Cytology and Organization.* New York: Springer-Verlag, 1974, p. 142–179.

Prybylowski K, Fu Z, Losi G, Hawkins LM, Luo J, Chang K, Wenthold RJ, and Vicini S. Relationship between availability of NMDA receptor subunits and their expression at the synapse. *J Neurosci* 22: 8902–8910, 2002.

Ragnarsson L, Yasuda T, Lewis RJ, Dodd PR, and Adams DJ. NMDA receptor subunit-dependent modulation by conantokin-G and Ala(7)-conantokin-G. *J Neurochem* 96: 283–291, 2006.

Rosenmund C, Clements JD, and Westbrook GL. Nonuniform probability of glutamate release at a hippocampal synapse. *Science* 262: 754–757, 1993.

Rumbaugh G, Prybylowski K, Wang JF, and Vicini S. Exon 5 and spermine regulate deactivation of NMDA receptor subtypes. *J Neurophysiol* 83: 1300–1307, 2000.

Rumbaugh G and Vicini S. Distinct synaptic and extrasynaptic NMDA receptors in developing cerebellar granule neurons. *J Neurosci* 19: 10603–10610, 1999.

Sasaki YF, Rothe T, Premkumar LS, Das S, Cui J, Talantova MV, Wong HK, Gong X, Chan SF, Zhang D, Nakanishi N, Sucher NJ, and Lipton SA. Characterization and comparison of the NR3A subunit of the NMDA receptor in recombinant systems and primary cortical neurons. *J Neurophysiol* 87: 2052–2063, 2002.

Silver RA, Traynelis SF, and Cull-Candy SG. Rapid-time-course miniature and evoked excitatory currents at cerebellar synapses in situ. *Nature* 355: 163–166, 1992.

Takada N, Yanagawa Y, and Komatsu Y. Activity-dependent maturation of excitatory synaptic connections in solitary neuron cultures of mouse neocortex. *Eur J Neurosci* 21: 422–430, 2005.

Takahashi T, Feldmeyer D, Suzuki N, Onodera K, Cull-Candy SG, Sakimura K, and Mishina M. Functional correlation of NMDA receptor epsilon subunits expression with the properties of single-channel and synaptic currents in the developing cerebellum. *J Neurosci* 16: 4376–4382, 1996.

Thomas CG, Miller AJ, and Westbrook GL. Synaptic and extrasynaptic NMDA receptor NR2 subunits in cultured hippocampal neurons. *J Neurophysiol* 95: 1727–1734, 2006.

Tovar KR and Westbrook GL. The incorporation of NMDA receptors with a distinct subunit composition at nascent hippocampal synapses in vitro. *J Neurosci* 19: 4180–4188, 1999.

Vallano ML, Lambolez B, Audinat E, and Rossier J. Neuronal activity differentially regulates NMDA receptor subunit expression in cerebellar granule cells. *J Neurosci* 16: 631–639, 1996.

Vicini S, Wang JF, Li JH, Zhu WJ, Wang YH, Luo JH, Wolfe BB, and Grayson DR. Functional and pharmacological differences between recombinant *N*-methyl-D-aspartate receptors. *J Neurophysiol* 79: 555–566, 1998.

Wang YH, Bosy TZ, Yasuda RP, Grayson DR, Vicini S, Pizzorusso T, and Wolfe BB. Characterization of NMDA receptor subunit-specific antibodies: distribution of NR2A and NR2B receptor subunits in rat brain and ontogenic profile in the cerebellum. *J Neurochem* 65: 176–183, 1995.

Watanabe M, Mishina M, and Inoue Y. Distinct spatiotemporal expressions of five NMDA receptor channel subunit mRNAs in the cerebellum. *J Comp Neurol* 343: 513–519, 1994.